Int J Thermophys (2009) 30:1118–1129
DOI 10.1007/s10765-009-0559-5

Thermal Conductivity and Phase Diagrams of Some Potential Hydrogen Storage Materials Under Pressure

Bertil Sundqvist · Ove Andersson

Received: 17 September 2008 / Accepted: 12 January 2009 / Published online: 31 January 2009

Abstract Experimental data for the thermal conductivity of the complex hydrides $NaAlH_4$, $LiBH_4$, $NaBH_4$, and KBH_4, in dense, solid form over wide ranges in temperature and pressure are presented. These materials contain high volume and mass fractions of hydrogen and are considered possible candidates as future hydrogen storage materials for mobile applications. The pressure–temperature phase diagrams of several materials as obtained from thermal-conductivity studies are briefly discussed, and the temperature and pressure dependencies of the thermal conductivity of the bulk materials are also discussed using simple theoretical models.

Keywords KBH_4 · $LiBH_4$ · $NaBH_4$ · $NaAlH_4$ · Phase diagram · Thermal conductivity

1 Introduction

The possibility to use hydrogen as an energy carrier in mobile applications has recently sparked large interest [1]. Because of the low density of condensed hydrogen, hydrogen-rich compounds have been suggested as primary candidates for hydrogen storage. The ideal compound should contain large volume and mass fractions of hydrogen, and should be able to store and release hydrogen by reversible processes in temperature and pressure regions considered safe by authorities and users. One type of compounds considered involves complex hydrides, which may contain up to 18 mass% hydrogen ($LiBH_4$), and in some cases, may reversibly take up and release hydrogen under controlled thermodynamic conditions.

In the design of thermally activated processes, knowledge of the thermal properties is obviously important. We have studied the thermal conductivities, κ, of several

B. Sundqvist (✉) · O. Andersson
Department of Physics, Umeå University, 901 87 Umeå, Sweden
e-mail: bertil.sundqvist@physics.umu.se

alanates and borohydrides as functions of pressure and temperature, using an accurate and reliable hot-wire method [2], and here we present and discuss experimental data for the thermal conductivity of several materials, $LiBH_4$, $NaBH_4$, KBH_4, and $NaAlH_4$, both at normal and elevated pressures. $LiAlH_4$ was recently predicted to have a structural transition near 2.5 GPa associated with an increase in density by 17 % [3], and we were able to verify the existence of a transition in this rather accessible pressure range [4]. Obviously, if such a dense high-pressure phase can be stabilized at atmospheric pressure, this will increase the storage capability of the material, and our measurements of κ have also been used to map structural phase diagrams from the observed anomalies at structural phase transformations. We therefore give some examples of interesting recent discoveries in this area. Finally, we discuss briefly upon the technological and practical values of the measured data.

2 Experimental Methods and Details

The materials were obtained in the form of powders from Sigma-Aldrich and Fischer Scientific, with stated purities varying from 90 % ($NaAlH_4$) to 99.9 % ($LiBH_4$ and KBH_4). All measurements were carried out under high pressures between 0.1 GPa and 2 GPa, using a piston and cylinder device with an internal diameter of 45 mm. The applied pressure compresses the original soft powder into a fully dense, polycrystalline material. The thermal conductivity was measured by a hot-wire method [2], which also gives data for the specific heat capacity, although with reduced accuracy. Because the sample extends only about 3 mm to 5 mm from the hot-wire, the temperature pulse may be reflected back to disturb the temperature field at the wire location and thus reduce the measurement accuracy. As discussed in the original paper [2], this can be observed in the quality of the fit of the theoretical time dependence to the data, and in our experiments, the effect usually begins to show at values for κ in the range of 5 $W \cdot m^{-1} \cdot K^{-1}$ to 7 $W \cdot m^{-1} \cdot K^{-1}$. In many such cases, the error in κ can still be kept below 3 % to 5 % by using only the initial part of the measured time series, although the data for c_p will be significantly less accurate. In some experiments, one thermocouple was embedded in the sample and a second one in the pressure cell wall to enable identification of the phase transformations also by differential thermal analysis (DTA). The thermally insulated pressure vessel could be cooled by liquid nitrogen to about 100 K or heated electrically. The large mass of the vessel ascertains slow changes in temperature and stable conditions. Most measurements have been carried out between 100 K and 300 K, but in some cases data have also been collected at elevated temperatures up to above 400 K.

3 Experimental Results and Discussion

3.1 Complex Alkali Metal Aluminum Hydrides

The light alkali metal aluminum hydrides are of very large interest, for several reasons. We mentioned above the existence of a dense high-pressure state above 2.5 GPa in $LiAlH_4$, which suggests the possibility to improve the volumetric storage properties

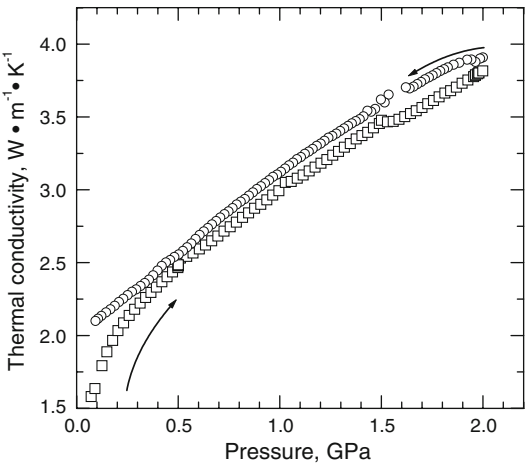

Fig. 1 Thermal conductivity of $NaAlH_4$ as a function of pressure at 293 K

of complex hydrides. Even more interesting, $NaAlH_4$ is known to reversibly store and release hydrogen under low-pressure–temperature conditions in the presence of Ti as a catalyst [5]. $NaAlH_4$ also has a denser high-pressure phase, but the transition pressure is very high, 13 GPa [6,7]. However, the hysteresis associated with this transition is enormous, about 10 GPa [6], indicating that metastable dense phases may exist at atmospheric pressure. (There are also indications of a possible small structural anomaly near 5 GPa [6,8], but the evidence is weak and few details are known.)

In order to check the stability of the lattice at low temperatures, we recently measured κ for $NaAlH_4$ up to 2 GPa in the range from 100 K to 300 K. The results presented in Figs. 1 and 2 show that no phase transitions exist in this range. In this experiment pressure was slowly increased at room temperature, and Fig. 1 shows a strong curvature in $\kappa(p)$ up to about 0.3 GPa, associated with densification of the powder sample. At 0.5 GPa, 1 GPa, 1.5 GPa, and 2 GPa, temperature runs were made to below 100 K. Figure 2 shows that at 0.5 GPa κ has a temperature dependence very close to the $\kappa = AT^{-1}$ expected for a pure insulating crystal in which κ is limited by three-phonon Umklapp interactions. This indicates that compression of the initial powder has resulted in a dense sample, and that defects, impurities, and grain boundaries play a much smaller role than might be expected, taking into account the low nominal purity and the large plastic deformation suffered by the material on compression. Because the mass ratio Na/AlH_4 is only about 1.35, we expect the lowest optical phonon branch to be effectively a continuation of the acoustic branch, with no obvious energy gap, and this is also clearly shown in recent calculations by Ke and Tanaka [9]. We thus do not expect any significant effects on $\kappa(T)$ due to the excitation of optical phonons [10,11]. At higher pressures, we notice an increase in the experimental scatter at low temperatures, and there is also a tendency toward a weaker temperature dependence than $\kappa \propto T^{-1}$, especially at 2 GPa. The appearance of these features is associated with an observed increase in the rms deviations between the measured temperatures and the fitted theoretical function, and as mentioned above, we identify these effects as arising from a reflection of the temperature pulse from the sample boundary.

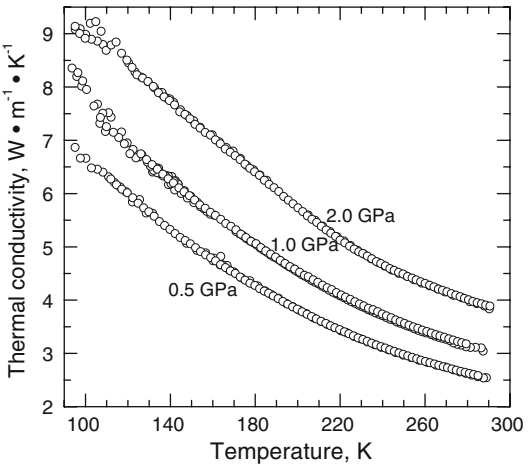

Fig. 2 Thermal conductivity of $NaAlH_4$ as a function of temperature at several pressures

The high accuracy and excellent thermal and geometrical stabilities in the experiment are well illustrated by the fact that after each low-temperature cycle, κ returns to almost exactly the same value as before the run near 293 K. This is evident from Fig. 1, where the measured pressure dependence has only very small discontinuities at the pressures where we carried out temperature runs. The pressure coefficient $d\ln\kappa/dp$ is about 0.58 GPa^{-1} near zero pressure at 293 K. Using the measured bulk modulus $B_0 = 20$ GPa [7], we find a volume dependence of $d\ln\kappa/d\ln V = -11.6$, which is an unusually large value. Using semi-classical approximations, the volume dependence of a phonon–phonon limited κ can be derived as [12]

$$d\ln\kappa/d\ln V = -3\gamma - 2(d\ln\gamma/d\ln V) + 1/3, \tag{1}$$

where $\gamma = -d\ln\Theta_D/d\ln V$ is the Grüneisen parameter and Θ_D is the Debye temperature. For most crystalline solids, $d\ln\kappa/d\ln V$ is negative with a magnitude of 6–10 [12]. The high value observed here indicates either that the material is unusually anharmonic with a strongly pressure-dependent Θ_D and/or γ, that some other strong scattering mechanism such as defect scattering decreases rapidly under pressure, or that there are strong changes in the phonon bands with pressure.

All pressure studies so far indicate that the light alanates show strong structural hysteresis effects, and their phase relations are thus not easily investigated. Although this fact is an obstacle for scientific studies, it may be a technical advantage, making the existence of metastable phases at low pressure highly probable.

3.2 Alkali Metal Borohydrides

The lightest borohydrides, $LiBH_4$ and $NaBH_4$, contain the highest mass fractions of hydrogen and have been quite well investigated the last few years. The pressure–temperature phase diagram of $LiBH_4$ was well investigated by DTA already by Pistorius [13], but most of the actual lattice structures were unknown until recently. $LiBH_4$

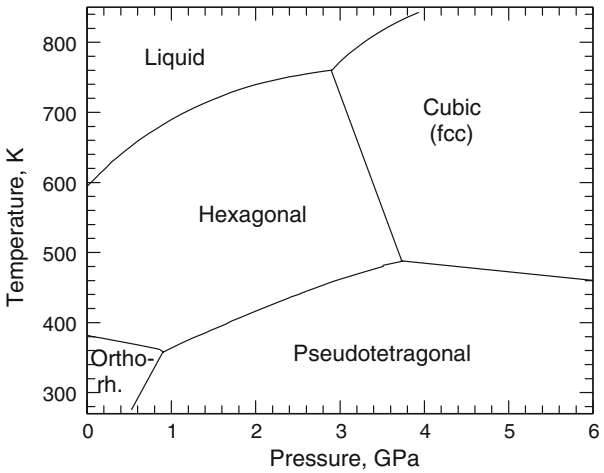

Fig. 3 Phase diagram of $LiBH_4$, based on the work of Pistorius [13] and Dmitiev et al. [14]

is unique among the borohydrides in having an orthorhombic structure at room temperature, transforming into hexagonal on heating above 380 K. The structures of the high-pressure phases were very recently identified by Dmitriev et al. [14], who showed that the low-temperature structure transforms into a pseudo-tetragonal lattice above 0.7 GPa, and then into a face-centered-cubic lattice at high temperatures or at very high pressures well above 10 GPa. A corrected version of Pistorius' phase diagram is shown in Fig. 3.

We have measured the thermal conductivity in the two low-temperature phases with the results shown in Fig. 4. For both phases, κ again shows a temperature dependence very close to the "normal" $\kappa(T) \propto T^{-1}$, showing that we have a good crystal structure with few imperfections and impurities and a relatively large grain size. The pressure dependence, shown in Fig. 5, is much more unusual. In the tetragonal high-pressure phase near 1 GPa, κ increases with increasing pressure with a rather "normal" pressure coefficient of $\mathrm{d}\ln\kappa/\mathrm{d}p \approx 0.29\,\mathrm{GPa}^{-1}$, but in the orthorhombic low-pressure phase, we find that the pressure coefficient of κ is close to zero, $\mathrm{d}\ln\kappa/\mathrm{d}p \approx 0.07\,\mathrm{GPa}^{-1}$. Using the recently determined bulk modulus $B_o = 14.4$ GPa [15], this corresponds to $\mathrm{d}\ln\kappa/\mathrm{d}\ln V = -1.0$, which is an extremely small value more reasonable for a glass than a crystalline material [12]. Although this fact might indicate that κ is limited by a very large disorder, this is clearly contradicted by the completely "normal" temperature dependence in Fig. 4. Instead, we must assume that the phonons involved in the thermal conduction are little affected by the change in volume, i.e., there is possibly a strong softening of some phonon branch(es) under pressure. This feature may be connected with the very strong hysteresis observed for this transition [13,14,16]. As discussed by Dmitriev et al. [14], the transition between the low-pressure phases of $LiBH_4$ that basically contain AB stacked double $LiBH_4$ planes, and the high-pressure phases with cubic ABC stacking, involves both a reshuffling and a distortion of the planes, and the transitions are indeed connected with phonon instabilities.

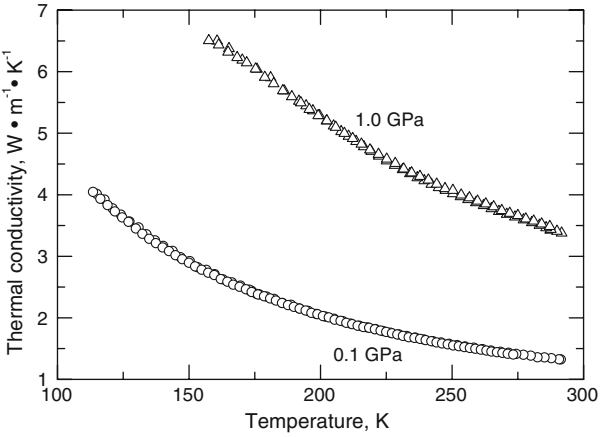

Fig. 4 Thermal conductivity of $LiBH_4$ at 0.1 GPa (rhombohedral phase) and 1 GPa (tetragonal)

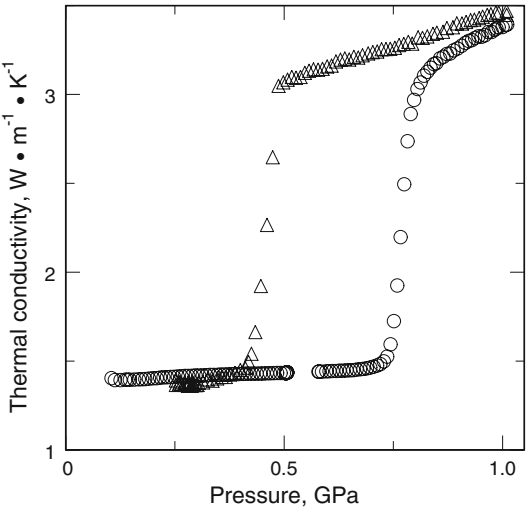

Fig. 5 Thermal conductivity of $LiBH_4$ versus pressure at 285 K: *circles*, increasing pressure, *triangles*, decreasing pressure

Figure 6 shows the low-temperature part of the phase diagram of $LiBH_4$, as found from our DTA and thermal-conductivity measurements. At room temperature and above, the hysteresis of the transition is quite large, at least 0.2 GPa (see Fig. 5). However, on further cooling, the orthorhombic-to-tetragonal transition pressure becomes almost independent of temperature, indicating that at low pressures the energy threshold for starting the transition exceeds the thermal energy. The reverse transition, on the other hand, follows a straight line in p–T space. The result is that the pseudo-tetragonal high-pressure phase can never be produced below about 0.6 GPa, but once formed, this phase is stable at atmospheric pressure at all temperatures below about 190 K. There may thus exist a possibility to stabilize a more dense $LiBH_4$ structure at low pressures for storage purposes.

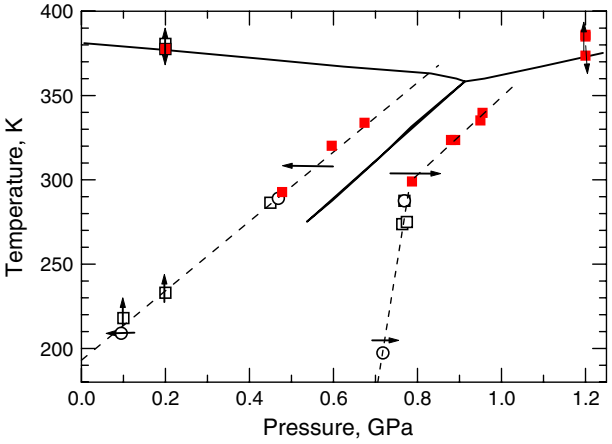

Fig. 6 Low-pressure phase diagram of $LiBH_4$. Squares denote anomalies observed by DTA, and *circles* by thermal conductivity. *Open* and *filled* symbols indicate different experiments. Full lines show "equilibrium" phase boundaries given by Pistorius [13], and *dashed lines* show phase boundaries for increasing and decreasing pressure (*arrows*) found in our experiments

In the high-temperature hexagonal phase, the borohydride tetrahedra are strongly disordered, and in this phase, the thermal conductivity is almost independent of temperature as would be expected if the phonon mean free path is limited to an almost constant value by a strong disorder scattering (see Fig. 5 of Ref. [14]). An extrapolation of the data for the room temperature orthorhombic phase shows that the thermal conductivities of the two phases found at atmospheric pressure are very similar near the phase boundary.

At atmospheric pressure all heavier borohydrides have a face-centered-cubic $Fm\bar{3}m$ structure with orientationally disordered BH_4 tetrahedra at room temperature. At low temperature, they transform into orientationally ordered tetragonal structures. For $NaBH_4$, this occurs at 190 K and involves a large step change in the thermal conductivity [17], as shown in Fig. 7. The temperature dependence of κ reflects the orientational order. While the low-temperature data are compatible with a fairly well-ordered crystal structure with $\kappa \propto T^{-0.65}$, the temperature dependence in the high-temperature disordered phase is significantly weaker, at $T^{-0.45}$. The pressure coefficient in this phase is also rather low at room temperature, $\mathrm{d}\ln\kappa/\mathrm{d}p = 0.20\,\mathrm{GPa}^{-1}$. With a bulk modulus of $B_0 = 20\,\mathrm{GPa}$ [18], this gives $\mathrm{d}\ln\kappa/\mathrm{d}\ln V = -4$. Like the weak temperature dependence, this rather low value (see above and Ref. [12]) probably reflects a significant disorder in the structure, such that the phonon mean-free path changes only slowly with temperature and pressure, but since the stated purity of the material was only about 98 %, there may also be a small impurity contribution to the thermal resistivity.

The data shown in Fig. 7 were used to identify and map the tetragonal-to-cubic transition in the low-pressure region [17]. Using structural data from other sources [18,19], we can extend the phase line to above 6 GPa at room temperature, as shown in Fig. 8. The phase diagram of $NaBH_4$ has recently been quite well investigated,

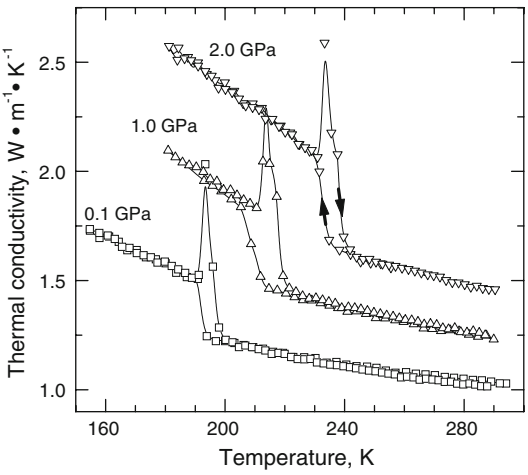

Fig. 7 Low-temperature thermal conductivity of $NaBH_4$ at the pressures indicated

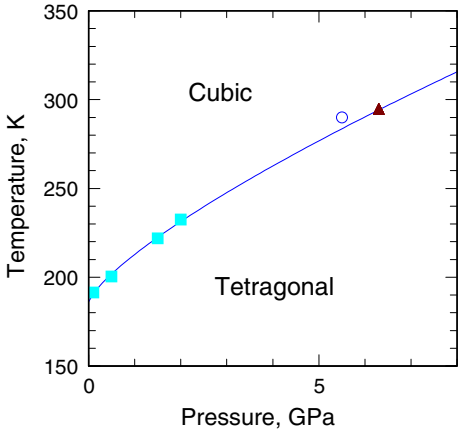

Fig. 8 Low-pressure phase diagram of $NaBH_4$: *squares* indicate points from thermal-conductivity data, *triangle* from Ref. [18], and *circle* from Ref. [19]

and the structure of a third phase found above 8 GPa [18–20] has been identified as orthorhombic [19].

Recently, there has also been an interest in the next heavier hydride, KBH_4, which is reported to have a low-temperature transition into a tetragonal phase at 76 K [21]. Kumar et al. [22] have recently found a phase evolution at room temperature which is very similar to that shown in Fig. 8 for $NaBH_4$. They find a transition into a tetragonal phase near 4 GPa and a further transition into an orthorhombic phase for this material near 6 GPa. In order to investigate the similarities and differences between the phase diagrams of $NaBH_4$ and KBH_4, we have recently measured the thermal conductivity of KBH_4 between 100 K and 400 K at pressures up to 2 GPa. Comparing the results for KBH_4 in Fig. 9 with those for $NaBH_4$ in Fig. 7, it is obvious that there is no discontinuity in the data for KBH_4 in the range investigated, and we thus do not observe any phase transformation into the ordered tetragonal phase. We also note that for KBH_4 the temperature dependence of κ is much stronger than the normal T^{-1} high-tem-

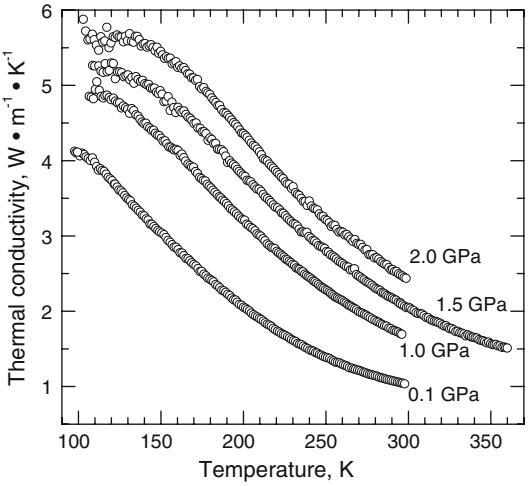

Fig. 9 Thermal conductivity of KBH_4 at the pressures indicated

perature behavior. At 0.1 GPa κ increases by almost a factor of three between 300 K and 150 K, which is close to $T^{-1.6}$. A similar behavior is seen at all pressures, and above 1 GPa, $\kappa(T)$ also shows a clear tendency to approach a maximum near 100 K and 5.5 $W \cdot m^{-1} \cdot K^{-1}$. At the lowest temperatures, we again see an increase in the experimental scatter caused by reflected temperature waves. (This can be seen very clearly in the deviations from the fitted temperature curves, as discussed above.)

We cannot completely rule out that the maximum in $\kappa(T)$ is an experimental artifact caused by the wave reflection effect, but it seems likely that we observe the normal impurity and defect scattering limited peak in κ. If this is correct, the very strong temperature dependence observed above 100 K is probably associated with the onset of strong phonon–phonon Umklapp scattering (with an exponential temperature dependence) near and above the expected maximum in $\kappa(T)$. The large mass ratio $K/BH_4 = 2.6$ should give a sizeable energy gap between optical and acoustic phonons, and in principle, a similar effect might arise in $\kappa(T)$ when optical phonons begin to be excited and start to scatter the acoustic phonons carrying the heat [10]. Such an effect is observed, for example, in first principles calculations on alkali halides by Pettersson [11]. However, here the observed temperature is too low for this effect to be a realistic alternative.

At room temperature, the thermal conductivity increases with increasing pressure as $d\ln\kappa/dp = 0.68\,GPa^{-1}$. The data in Fig. 10 show a tendency for κ to increase faster with pressure at higher pressures, probably reflecting the fact that the peak in κ (Fig. 9) moves to higher temperatures under pressure. Such an effect would indeed be expected if the peak is due to the onset of Umklapp scattering, as mentioned above, since the increasing size of the Brillouin zone under pressure would push the Umklapp limit to higher energies, and thus higher temperatures. With the experimental bulk modulus of $B_0 = 16.8\,GPa$ [22], we find $d\ln\kappa/d\ln V = -11.4$. This is again a rather high value but in reasonable agreement with data for other pure insulating materials [12].

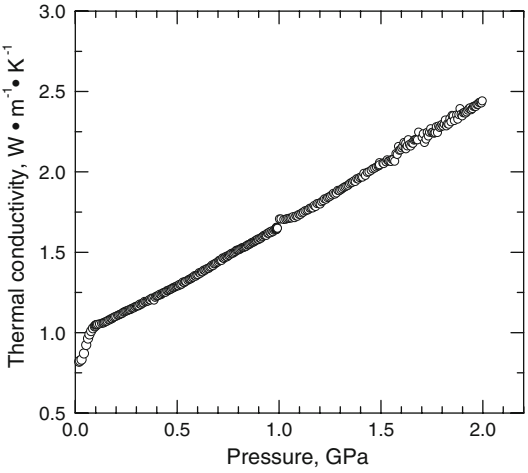

Fig. 10 Thermal conductivity of KBH_4 as a function of pressure at room temperature

We were surprised not to observe any clear indications of a transformation into the orientationally ordered tetragonal phase at low temperature at the highest pressures. Both the data for $NaBH_4$ (Fig. 7) and consideration of the scattering mechanisms indicate that κ should become higher in the tetragonal phase, and in principle, we can imagine that the very strong increase observed in κ between 100 K and 200 K corresponds to a gradual ordering, i.e., a strongly smeared transition. However, even in such a case, we expect the temperature dependence to turn into the typical T^{-1} dependence below the transition, and this is not seen. We thus conclude that there is no such transition at or above 120 K below 2 GPa. The absence of this transition has interesting implications for the phase diagram. Kumar et al. [22] observe a transition into a tetragonal phase at 4 GPa near 290 K, but the data in Fig. 9 eliminate the possibility that Kumar's tetragonal phase is identical to the low-temperature phase. Even if the phase line would be straight instead of curved toward the pressure axis as shown in Fig. 8, a zero-pressure transition at 76 K [21] gives a transition pressure above 8 GPa at room temperature. If we assume a very strong temperature hysteresis for this transition, we can possibly decrease this number, but not by the necessary factor of two. We thus conclude that the tetragonal phase observed by Kumar et al. cannot be identical to the tetragonal low-temperature phase.

4 Conclusions and Final Comments

We have shown above that measurements of the thermal conductivity give very good possibilities to identify structural changes and map the pressure–temperature phase diagrams of the complex hydrides. Such phase diagrams may be of large value when trying to design better hydrogen storage materials. For example, it may be possible to identify dense structural phases which may be stabilized at low pressures by the introduction of suitable impurities. Such work is already under way; quite recently, the

Table 1 Measured thermal conductivities (in $W \cdot m^{-1} \cdot K^{-1}$) extrapolated to atmospheric pressure for several complex hydrides at selected temperatures

	100 K	150 K	200 K	250 K	300 K
$NaAlH_4$	5.35	4.14	3.13	2.39	1.94
$LiBH_4$	4.40	2.89	2.03	1.54	1.23
$NaBH_4$	–	1.70[a]	1.18[b]	1.07[b]	1.00[b]
KBH_4	4.02	2.90	1.93	1.29	0.96

[a] Tetragonal phase (below 190 K)
[b] Cubic phase

first mixed alkali metal borohydride $LiK(BH_4)_2$ was synthesized and characterized structurally [23].

The data obtained for κ are also of scientific and technological value in themselves, and in Table 1 we give numerical data for the thermal conductivity κ as a function of temperature for the four hydrides studied. As already discussed above, the data can be well understood using simple theoretical ideas for ordered and disordered polycrystalline insulators.

Finally, we stress that the data presented in this article are valid for the fully hydrogenated dense polycrystalline materials in their normal structural states only. No measurements have been carried out in the technologically interesting high-temperature regime where hydrogen release can be expected. With the present system, using a Ni or Pt hot-wire, measurements are not possible in the presence of free hydrogen at high temperature because the wire would be rapidly destroyed by reaction with the hydrogen. In this range, we expect the thermal conductivity of the solid bulk material to be significantly lower than indicated by our measurements because of the rapidly increasing number of hydrogen vacancies and the disorder created by the reaction process. A reasonable estimate of κ in this regime can probably be obtained using Slack's [10] theory for the minimum thermal conductivity, or simply by inserting a mean-free path λ of the order of the lattice constant in the semi-classical formula $\kappa = (1/3)c_v v_s \lambda$, where v_s is the speed of sound and c_v is the specific heat capacity. We must also point out that in a real storage system containing a packed powder, the main heat transport is probably mediated by the hydrogen gas surrounding the solid grains, and the thermal properties of such a bed are probably quite different from the average properties of the individual solid grains. This is also evident from the recent studies of such packed $NaAlH_4$ powder beds by Dedrick et al. [24].

Acknowledgment This study was financially supported by Carl Tryggers Stiftelse för Vetenskaplig Forskning and Magn. Bergvalls Stiftelse.

References

1. L. Schlapbach, A. Züttel, Nature **414**, 353 (2001)
2. B. Håkansson, P. Andersson, G. Bäckström, Rev. Sci. Instrum. **59**, 2269 (1988)
3. P. Vajeeston, P. Ravindran, R. Vidya, H. Fjellvåg, A. Kjekshus, Phys. Rev. B **68**, 212101 (2003)

4. A.V. Talyzin, B. Sundqvist, Phys. Rev. B **70**, 180101 (2004)
5. B. Bogdanovich, M. Schwickardi, J. Alloys Compd. **253**, 1 (1997)
6. A.V. Talyzin, B. Sundqvist, High Pressure Res. **26**, 165 (2006)
7. S. Nakano, A. Nakayama, K. Takemura, in *Proceedings of Joint 20th AIRAPT and 43rd EHPRG Conference on High Pressure Science and Technology*, ed. by E. Dinjus, N. Dahmen (Forschungszentrum Karlsruhe, Karlsruhe, 2005), ISBN 3-923704-49-6, paper T5-P027; available at http://www.unipress.waw.pl/airapt/AIRAPT-20/html/proceedings/index.html
8. B. Sundqvist, O. Andersson, A.V. Talyzin, J. Phys.: Condens. Matter **19**, 425201 (2007).
9. X.Z. Ke, I. Tanaka, Phys. Rev. B **71**, 024117 (2005)
10. G.A. Slack, in *Solid State Physics*, vol. 34, ed. by H. Ehrenreich, F. Seitz, D. Turnbull (Academic Press, New York, 1979), p. 1
11. S. Pettersson, J. Phys. C **21**, 1727 (1988)
12. R.G. Ross, P. Andersson, B. Sundqvist, G. Bäckström, Rep. Prog. Phys. **47**, 1347 (1984)
13. C.W.F.T. Pistorius, Z. Phys. Chem., Neue Folge **88**, 253 (1974)
14. V. Dmitriev, Y. Filinchuk, D. Chernyshov, A.V. Talyzin, O. Andersson, A. Dzwilewski, B. Sundqvist, A. Kurnosov, Phys. Rev. B **77**, 174112 (2008)
15. Y. Filinchuk, D. Chernyshov, A. Nevidomskyy, V. Dmitriev, Angew. Chem. Int. Ed. **47**, 529 (2008)
16. A.V. Talyzin, O. Andersson, B. Sundqvist, A. Kurnosov, L. Dubrovinsky, J. Solid-State Chem. **180**, 510 (2007)
17. B. Sundqvist, O. Andersson, Phys. Rev. B **73**, 092102 (2006)
18. R.S. Kumar, A.L. Cornelius, Appl. Phys. Lett. **87**, 261916 (2005)
19. Y. Filinchuk, A.V. Talyzin, D. Chernyshov, V. Dmitriev, Phys. Rev. B **76**, 092104 (2007)
20. C.M. Araújo, R. Ahuja, A.V. Talyzin, B. Sundqvist, Phys. Rev. B **72**, 054125 (2005)
21. G. Renaudin, S. Gomes, H. Hagemann, L. Keller, K. Yvon, J. Alloys Compd. **375**, 98 (2004)
22. R.S. Kumar, E. Kim, A.L. Cornelius, J. Phys. Chem. C **112**, 8452 (2008)
23. E.A. Nickels, M.O. Jones, W.I.F. David, S.R. Johnson, R.L. Lowton, M. Sommariva, P.P. Edwards, Angew. Chem. Int. Edit. **47**, 2817 (2008)
24. D.E. Dedrick, M.P. Kanuoff, B.C. Replogle, K.J. Gross, J. Alloys Compd. **389**, 299 (2005)